191st ELECTROCHEMICAL SOCIETY MEETING, MONTREAL, QUEBEC, CANADA (May 4-9, 1997)

BNL-64662

UNDERPOTENTIAL DEPOSITION OF Ag ADLAYERS ON Pt(111): STRUCTURES AND DETERMINATION OF O_2 ADSORPTION ON Pt(111)

CONF-970517--

N.S. Marinković, J.X. Wang and R.R. Adžić

Chemical Sciences Division, Department of Applied Science
Brookhaven National Laboratory, Upton NY 11973

ABSTRACT

The structure of Ag adlayers deposited at underpotentials in sulfuric acid on Pt (111), and the inhibition of O_2 reduction they cause, have been studied using grazing incident angle x-ray diffraction measurements, as well as linear sweep voltammetry and *in situ* FTIR spectroscopy. Ag forms a hexagonal incommensurate bilayer, with two mutually commensurate monolayers. It is aligned with the Pt(111) substrate, although slightly expanded. The first monolayer has a commensurate (1x1) structure. A second layer causes a restructuring of the first monolayer. Deposition of each monolayer is associated with one voltammetry peak. A complete inhibition of O_2 reduction on Pt(111) has been observed upon deposition of both, Ag monolayer and bilayer. Analysis of the inhibition of O_2 reduction as a function of the Ag coverage shows that during reduction O_2 adsorbs in a bridge configuration on Pt(111).

INTRODUCTION

The underpotential deposition (UPD) of Ag on Pt has recently attracted a considerable interest (1,2,3,4,5,6,7). Despite new insights into the behavior of this system, it is not yet fully understood. A formation of two monolayers at underpotentials is interesting feature of this system. In addition, unlike many other metal adatoms that have small or negligible effects on O_2 reduction on Pt, Ag causes a complete inhibition of this reaction (for review see references 8). In this work, surface X-ray scattering (SXS) and Fourier transform infrared spectroscopy (FTIR) techniques were used to characterize the UPD of Ag on Pt(111) electrode in sulfuric acid solution. SXS technique is particularly suitable for characterization of two layers of Ag before bulk deposition, which is not possible by scanning probe techniques. Structural information obtained by SXS technique was used to analyze the inhibition of O_2 reduction produced by the Ag adatoms. This inhibition provides a possibility to use these adatoms as a probe of adsorption reactions on electrode surfaces, with the position of Ag adatoms on Pt(111) verified by SXS measurements during the course of reaction. The type of O_2 adsorption on the Pt electrode surfaces has been a long-standing question of oxygen electrocatalysis. No distinction between the three models of O_2 adsorption, viz., Pauling (on-top, single bond), Griffths (on-top, double bond) and "bridge", could have been made so far.

EXPERIMENTAL

Platinum disks (3 mm by 10 mm and 6mm x 6mm) were aligned, polished and annealed as previously reported. The electrochemical-x-ray scattering cell was described in reference (9). The solutions were prepared from Ag_2SO_4 or $AgNO_3$ (Aldrich) and H_2SO_4 (SeaStar) and Milipore QC UV Plus water (Milipore Inc.). At a potential slightly positive of Ag deposition potential, the cell was deflated which leaves a thin 10μm-thick capillary electrolyte film between the Pt(111) face and the Prolene x-ray window. A reversible hydrogen electrode in Ag-free solutions was used as a reference electrode. The potentials are given with respect to standard hydrogen electrode (S.H.E.). Rotating hanging meniscus electrode measurements were carried out with a crystal 6mm in diameter, 6mm long. The rotator (Pine Instrument Co.) was fitted with a collet crystal holder which is similar to the one described earlier (10).

SXS measurements were carried out at the National Synchrotron Light Source (NSLS) at beam line X22B with $\lambda = 1.54$Å. A full description of the electrochemical SXS technique has been presented elsewhere (9). For Pt(111) it is convenient to use a hexagonal coordinate system in which $Q = (a^*,b^*,c^*) \times (H,K,L)$, where $a^* = b^* = 4\pi/\sqrt{3}a = 2.614$Å^{-1}, $c^* = 2\pi/\sqrt{6}a = 0.924$Å^{-1}, and $a = 2.775$ Å. The in-plane diffraction measurements were carried out in the (H,K) plane with L=0.2 corresponding to a grazing angle of 1.25 degree.

In situ spectroeletrochemical measurements were done in a cell described earlier (11). 4096 scans are coadded with parallel polarized light at sample and reference potentials using potential-step technique. Spectra are presented in $-\Delta R/R$ form, so that positive-going bands represent a gain of a particular species.

RESULTS AND DISCUSSION

Voltammetry of the UPD of Ag on Pt(111) in H_2SO_4 Solutions

Fig. 1 shows a linear potential voltammetry curve for the UPD of Ag on Pt(111) in 0.05M H_2SO_4 containing 1mM Ag^+. Two pronounced peaks in the anodic sweep occur at potentials 0.73 and 1.08V. The corresponding peaks in cathodic direction occur at 0.68 and 1.06V. These peaks are usually ascribed to a deposition of two Ag monolayers. The charge calculated from the voltammetry curve corresponds to 249μC/cm^2 for the peak at 1.1V and 261μcm^2 for the peak at 0.68V. These charges are close to the value of 240μC/cm^2 which corresponds to a full monolayer of Ag. The x-ray diffraction measurements, presented below, also show a formation of a Ag bilayer with one monolayer associated with each peak.

Previous voltammetry studies pointed out a problem of the instability of Pt(111) at high anodic potentials in the UPD of Ag (12). With the well-ordered Pt(111) in sulfuric acid solutions this does not appear as a problem since a strong adsorption of bisulfates prevents the oxidation of Pt at potentials of Ag dissolution.

DISCLAIMER

SXS Measurements

Grazing incident angle x-ray diffraction measurements were performed in order to determine the surface structure of electrodeposited silver adlayers in the absence and in the presence of O_2. Fig. 2 shows typical in-plane diffraction scans along K direction at two different potentials. At 0.85 V, there is a diffraction peak only at the integer position (0, 1, 0.3). This peak is very weak compared to that measured at 1.05 V with no Ag adatoms on the Pt(111) surface. The electron density of Ag is nearly half that of Pt, and the intensity of the (0, 1, 0.3) reflection, which is close to the anti-Bragg position, (0, 1, 0.5) along the (0, 1) non-specular rod, is expected to decrease upon formation of a pseudomorphic Ag monolayer. This is indeed observed experimentally which means that Ag forms a commensurate (1x1) monolayer on Pt(111) at potentials between the two voltammetry peaks. At 0.65V, negative of the second peak, additional diffraction peaks were found at (0, 0.940), (0, 0.940), (0.940, 0.940), (0, 1.880) and (1.880, 0). This diffraction features indicate the formation of an aligned hexagonal bilayer with the lattice constant of 2.952 ± 0.003 Å which is larger than that of bulk Ag. The question of the unusual expansion of the Ag incommensurate bilayer on Pt(111) will be discussed elsewhere (13). A second layer causes a restructuring of the first monolayer. From the observed in-plane diffraction pattern, and the intensity profile of the surface rods, it was found that the two adlayers are mutually commensurate (13). The Ag bilayer is stable after removing Ag^+ ions from the solution. The diffraction pattern and the real space model derived from it are shown in Fig. 3.

Oxygen Reduction on Pt(111) / Ag

Structural information on the foreign metal adlayers provide a possibility for a more complete study of their electrocatalytic effects in various reactions and their use as a probe of adsorption processes at electrode surfaces. To obtain such information requires monitoring the adlayer structure during the course of the reaction. It can be achieved by utilizing *in situ* SXS technique (14,15). Some limitations imposed by the cell construction imposed on the use of this technique in such measurements were discussed elsewhere (14). Limitation for O_2 reduction appear to be minor since it can be brought by diffusion through a thin Prolene film covering the cell perpendicular to the surface being investigated. There is, however, a problem of the current distribution. The current at the edge of the electrode is certainly larger than at the center of the front face of the crystal when counter electrode is around the crystal. This apparently does not cause a problem at small current densities which is the case with this reaction. It has been shown that the structure of the structure of Tl adlayer vanishes with O_2 reduction, but recovers when O_2 is replaced by N_2 (14,15). This shows that the reaction occurs predominantly at the front surface.

Fig. 4 shows O_2 reduction on Pt(111) obtained with a hanging meniscus rotating disk electrode in the absence and in the presence of the Ag adlayers. The curve for Pt(111) is in agreement with the literature data (16,17,18). The Ag monolayer causes a complete

inhibition of O_2 reduction. The reduction is also inhibited by the Ag bilayer. This may not be surprising, given very negative potentials of the reaction on bulk silver. The reaction on a Ag monolayer in solution containing no Ag^+ ions shows that the O_2 reduction starts at potential of 0.25V, which is more negative than on bulk Ag(111). O_2 reduction undergoes a four-electron reduction on bulk Ag and exhibits a small structural dependence (19). In acid solutions O_2 reduction starts at ~0.3V, which is considerably more negative than on Pt.

Fig 5 shows the effect of O_2 on the intensity of the diffraction peak at (0,0.94) position in the presence of Ag^+ in solution. A comparison with the measurement in the absence of O_2 at 0.7V shows a negligible decrease of the diffraction intensity. In the absence of Ag^+ in solution, O_2 reduction occurs at 0.2 V and causes a considerable decrease of the diffraction intensity. The peak position is unchanged which means that the Ag coverage and the adlayer structure remains unchanged in O_2 reduction (Fig. 4). This decrease in the diffraction intensity is similar to the decrease observed during O_2 reduction on the hexagonal Tl adlayer on Au (111) (14). This was ascribed to a decrease of the two-dimensional order of the adlayer, which decreases the diffraction intensity. These measurements indicate that the structure of Ag submonolayers is not changed during the course of O_2 reduction.

In situ FTIR spectroscopy measurements

Another possible explanation of the inhibition of O_2 reduction is a strong adsorption of bisulfate anions on Ag adlayer. A strong adsorption of tetrahedral bisulfate on Pt(111) is well established (20). Fig. 6 displays Fourier Transform Infrared Spectroscopy (FTIR) spectra obtained *in situ* 50mV apart, starting at 0.7V and using the reference potential of 0.68V, the potential of a bilayer formation. Bisulfate is adsorbed on the monolayer as indicated by the potential-dependent band at ~ 1200 cm^{-1}. Upon dissolution of Ag, a band for bisulfate adsorption on Pt becomes pronounced. A solution phase sulfate band, caused by anion migration and changes of the sulfate/bisulfate equilibrium due to bisulfate adsorption, is seen at 1100 cm^{-1}. A presence of a strong bipolar surface bisulfate band in the potential region $0.7V \leq E \leq 0.95$ V shows that the bisulfate adsorption on the bilayer is smaller than at the Ag monolayer. Coadsorption of sulfate/bisulfate was observed for Ag monolayer on Au(111) electrode (21). In HF and triflourmethane sulfonic acids, which have no specifically adsorbed anions , inhibition of O_2 reduction indicates that anion adsorption is not the cause. This is supported by a pronounced inhibition caused by small and intermediate Ag coverage which cannot adsorb tetrahedral anions.

Model of the site - blocking for O_2 adsorption by Ag adatoms

The essential first step in electrocatalytic O_2 reduction is its adsorption on the electrode surface, M, *viz.*,

$$O_2 + M = M - O_2(ads) \qquad [1]$$

The absence of this step would preclude O_2 reduction, unless the reaction can occur by an outer sphere charge transfer. The lack of O_2 reduction currents on the Ag/Pt(111) surface shows that the outer-sphere charge transfer is not operative at the potentials investigated. It is assumed that the O_2 adsorbs in a bridge configuration at Pt since it is conducive to a splitting of the O_2 molecule and ensuing four-electron reduction (22). There is no spectroscopic method to provide *in situ* information on O_2 adsorption. The inhibition by Ag adatoms can provide some information on this question of a considerable importance for oxygen electrocatalysis. The use of metal adatoms as a probe of adsorption processes was demonstrated on several examples (8, 23).

The measurements of the inhibition of O_2 reduction by Ag adatoms were carried out with Pt(111) as a function of the Ag coverage in the absence of Ag^+ ions in solution. Ag was adsorbed by exposing the Pt(111) crystal to N_2-saturated solutions containing various concentrations of Ag^+ for short times. The Ag coverages were determined in a separate cell and excess of Ag desorbed. Figs. 7 shows O_2 reduction as a function of Ag coverages. A very large decrease of the O_2 reduction current at small Ag coverages is observed.

In order to determine type of O_2 adsorption on the Pt(111) electrode surface, a model of the site-exclusion by Ag atoms is needed. A pronounced inhibition observed indicates that at least the near-neighbors Pt atoms must be affected by Ag adatoms. Fig. 8 shows the models for the site blocking by one Ag atom for adsorption of O_2 in a bridge (a) and in an on-top (b) configuration. Ag atom adsorbed in the hollow site blocks five bridge sites for O_2 adsorption. Only three sites are blocked for on-top adsorption. Conversely, five three-fold symmetry sites for Ag adsorption have to be unoccupied to form ensemble of Pt atoms for adsorption of one O_2 molecule at the bridge site. Likewise, three hollow sites have to be free from Ag for adsorption of O_2 at the top site. Protopopoff and Marcus (24) analyzed a range of possible effects of adsorbed sulfur on H_2 adsorption and evolution using similar approach.

This system can be treated quantitatively by using simple statistical treatment. If n is the number of O_2 sites blocked by one adsorbed Ag atom, an O_2 molecule can adsorb at a particular site only if n Ag sites are not occupied by Ag adatoms. The number of distinguishable ways in which q indistinguishable single particles are arranged on a lattice of N equivalent sites is given by (25,26),

$$W(q,N) = \binom{N}{q} = N! / (N - q)!\, q! \qquad (2)$$

The ensemble of Pt sites, which has to be unoccupied by Ag in order for O_2 to adsorb in a bridge, position occurs $\binom{N-5}{q}$ times since on the remaining (N - 5) hollow sites, q indistinguishable Ag atoms must be arranged. The probability of having such a structure

is

$$P = \binom{N-5}{q} / \binom{N}{q} \qquad [3]$$

By defining the Ag coverage by $\theta = q / N$, and assuming N is very large, the equation results into a simple expression $P = (1 - \theta)^5$, or at low coverages, $P = (1 - 5\theta)$. The slope of the initial part of this function at small coverages is -5. For the case of the on-top O_2 adsorption, the corresponding function will have the $(1 - \theta)^3$ and the slope for the inhibition at low Ag coverage would be -3. The plot of the normalized current for O_2 reduction on Pt(111) as a function of the Ag coverage at four different potentials is given in Fig. 9. The slope of the curve defined by points at small coverages is approximately -5. The calculated slope is given by dashed line. Therefore, the data in Fig. 9 provide first evidence, albeit indirect, for the bridge adsorption of O_2 on Pt(111) during the reduction in acid solutions. Gas phase adsorption data at 150K indicate a presence of a bridge and of on-top configurations (27). Chan et al. (28), using molecular orbital calculations, concluded that O_2 chemisorption on Pt(111) is favored at the two-fold site.

CONCLUSIONS

The UPD of Ag on Pt(111) represents an interesting UPD system which involves a bilayer formation before bulk Ag deposition. Ag forms a hexagonal incommensurate bilayer at underpotentials while the first monolayer has a commensurate (1x1) structure. Ag adatoms at coverages ≤ 1 reside in the three-fold symmetry hollow sites. The mutual commensurability of the two adlayers constituting a bilayer, and a small bilayer expansion with respect to the Pt(111) substrate, is important information about metal adlayers that can be obtained only with the SXS. The data presented above illustrate the usefulness of the structural information in studies of electrocatalytic reactions. In addition, they confirm the unique possibility of the SXS technique for determining the structure of electrode surfaces during the course of electrochemical reactions. The evidence was found for the O_2 adsorb in a bridge configuration on Pt(111), derived from the data on the inhibition of O_2 reduction by silver adatoms.

ACKNOWLEDGEMENTS

The authors thank S. Feldberg and B. Ocko for useful discussions. This research was performed under the auspices of the US Department of Energy, Division of Chemical Sciences and Materials Sciences Division, Office of Basic Energy Sciences under Contract No. DE-AC02-76CH00016.

REFERENCES

1. G.W. Tindal and S. Bruckenstein, Electrochim. Acta, **16**, 245 (1971).
2. S. Stucki, J. Electroanal. Chem., **80,** 375 (1977).
3. T. Chierchie, C. Mayer, K. Juttner, and W.J. Lorenz, J. Electroanal. Chem., **191,** 401 (1985).
4. P.B. Costa, J. Canullo, D.V. Moll, R.C. Salvarezza, M.C. Giordanno and A.J. Arvia, J. Electroanal. Chem., **244,** 261 (1988).
5. F.El Omar, R. Durand and R.Faure, J. Electroanal. Chem., **160,** 385 (1984).
6. N. Kamizuka and K. Itaya, Farad. Disc. **94**, 117 (1992).
7. A. Vashkevich, M. Rosenblum and E. Gileadi, J. Electroanal. Chem. **383**, 167 (1995).
8 R.R.Adzic, in Advances in Electrochemistry and Electrochemical Engineering, vol. 13, H. Gerischer and C. Tobias, Editors, p. 159 John Wiley, New York, 1984.
9. J.Wang, B.M. Ocko, A.J. Davenport and H.S. Isaacs, Phys. Rev. B **46**, 10321 (1992); B.M. Ocko, J.Wang, A.J. Davenport and H.S. Isaacs, Phys. Rev. Lett. **65**, 1466 (1990).
10. B.D. Cahan and H.M.Villulas, J. Electroanal. Chem., **307**, 263 (1991).
11 P.W. Faguy and N.S. Marinkovic, Anal. Chem., **67**, 2791(1995).
12. J.F. Rodriguez, D.L. Taylor and H.D. Abruna, Electrochim. Acta, **38,** 235 (1993).
13. J.X.Wang, N.S. Marinkovic, R.R. Adzic, B.M. Ocko,. Phys. Rev. Lett. submitted for publication.
14. R.R. Adzic, J.X. Wang, B.M. Ocko, Electrochim. Acta, **40,** (1995) 83.
15. R.R. Adzic, J.X. Wang, in "Oxygen Electrochemistry", R.R. Adzic, F.C. Anson, K. Kinoshita, Editors, **PV 95-26**, p. 61The Electrochemical Society Proceedings Series, Pennington NJ (1996).
16 N.M. Markovic, H. Geistarger and P.N.Ross, J. Phys. Chem., **99**, 3411 (1995).
17 F. El Kadiri,R.Faure, R. Durant, J.Electroanal. Chem., **301**, 177 (1991).
18 N.M. Markovic, R.R. Adzic, B.D. Cahan and E.B. Yeager, J. Electroanal. Chem., **377**, 249 (1994).
19. See e.g. R.R. Adzic, in Modern Aspects of Electrochemistry, vol.21, p. 163, R.E. White, J.O'M. Bockris and B.E. Conway Editors, Plenum Press (1990) New York.
20. P.W. Faguy, N.M. Markovic, R.R. Adzic, C.A. Fierro, E. B.Yeager, J. Electroanal. Chem., **289**, 245 (1990); P.W.Faguy, N.S. Marinkovic, R.R. Adzic, J. Electroanal. Chem., **407,** 209 (1996).
21. P. Mrozek, Y.-E. Sung, A. Wieckowski, Surf. Sci., **335**, 44 (1995).
22 E.Yeager, M.Razaq, D. Gervasio, A. Razaq, D. Tryk, J. Serb. Chem. Soc., **57**, 819 (1992).
23. R.R. Adzic, B.Z. Nikolic, F. Feddrix and E.Yeager, J.Electroanal. Chem., **341**, 287 (1992).

24 E. Protopopoff, P. Marcus, J. Chim. Phys., **88**, 1423 (1991).
25. E.Miyazaki and I. Yasumori, J. Math. Phys., **18**,215 (1977).
26. G.A. Martin, in Metal-Support and Metal-Additives Effects in Catalysis, B.Imelik et al. Editors, Elsevier, Amsterdam (1982).
27. H. Steininger, S. Lehwald and H. Ibach, Surf. Sci., **123**, 1 (1982).
28. A.W.E. Chan, R. Hoffman and W. Ho, Langmuir, **8**, 1111 (1992).

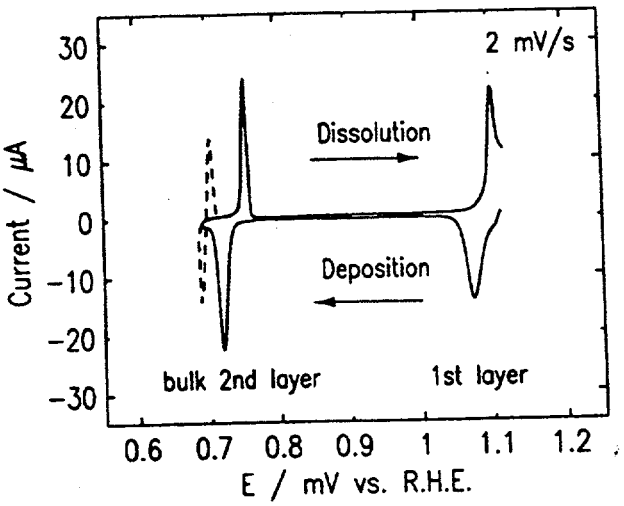

Fig. 1 Voltammetry curve for the UPD of Ag on Pt(111) in 0.05m H_2SO_4 with 1mM Ag^+. Sweep rate 2mV/s.

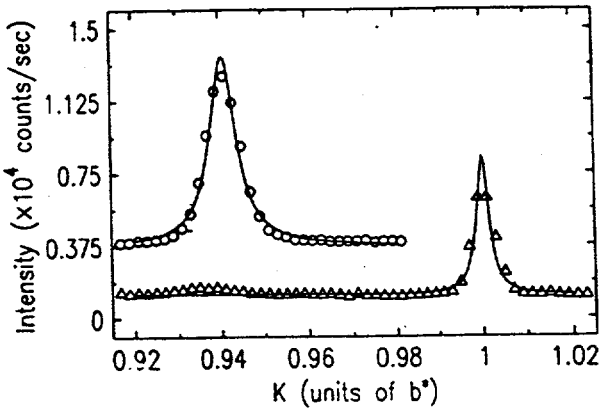

Fig. 2 In-plane diffraction scans along the (0,K,0.3) axis from on Pt(111) in 0.05M H_2SO_4 with 1mM Ag^+. Solid lines are the fits to a Lorenzian line shape.

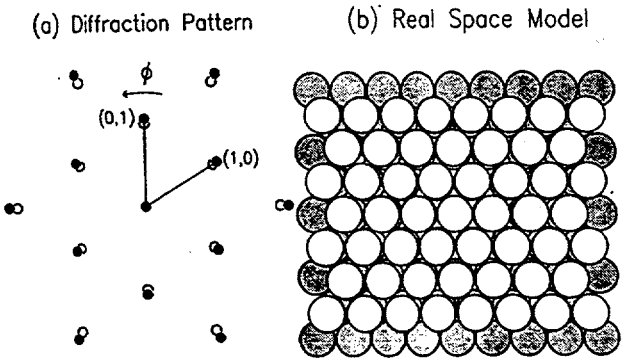

Fig. 3 In-plane diffraction pattern from Pt(111) in 0.05m H_2SO_4 with 1mM Ag^+ at 0.65V and the corresponding real space model of the Ag bilayer .

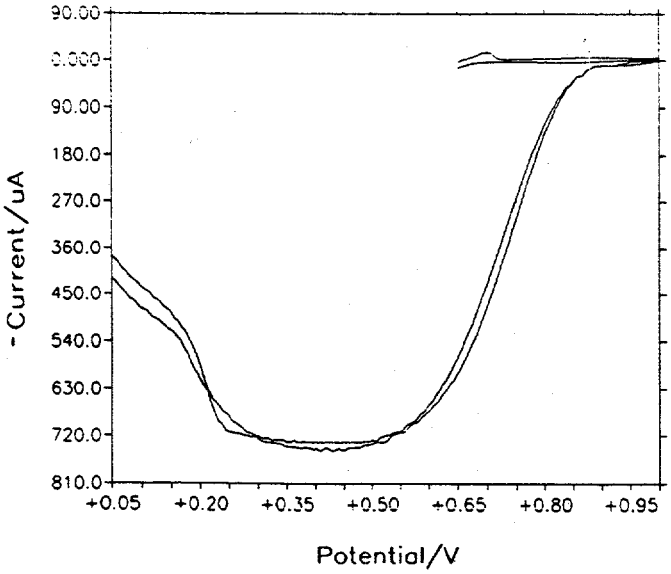

Fig. 4 O_2 reduction on a rotating hanging meniscus Pt(111) with and without Ag monolayer.900 rpm; 50mV/s.

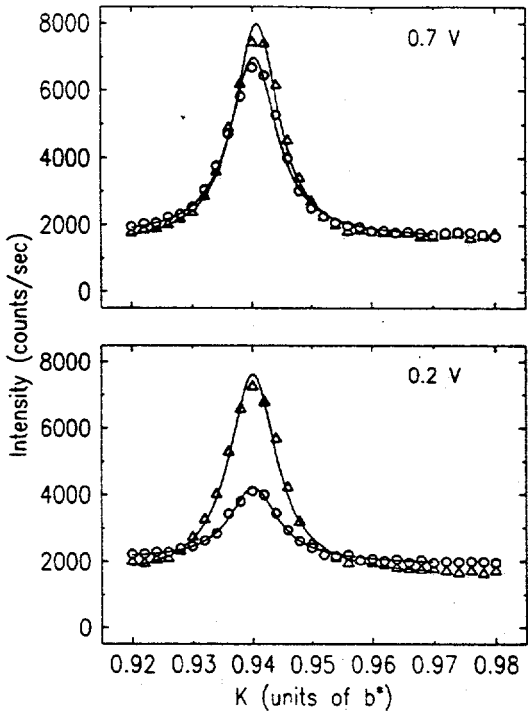

Fig. 5 In-plane diffraction scans along the (0,K,0.3) axis from on Pt(111) at indicated potentials in the absence (△) and in the presence of O_2 (○).

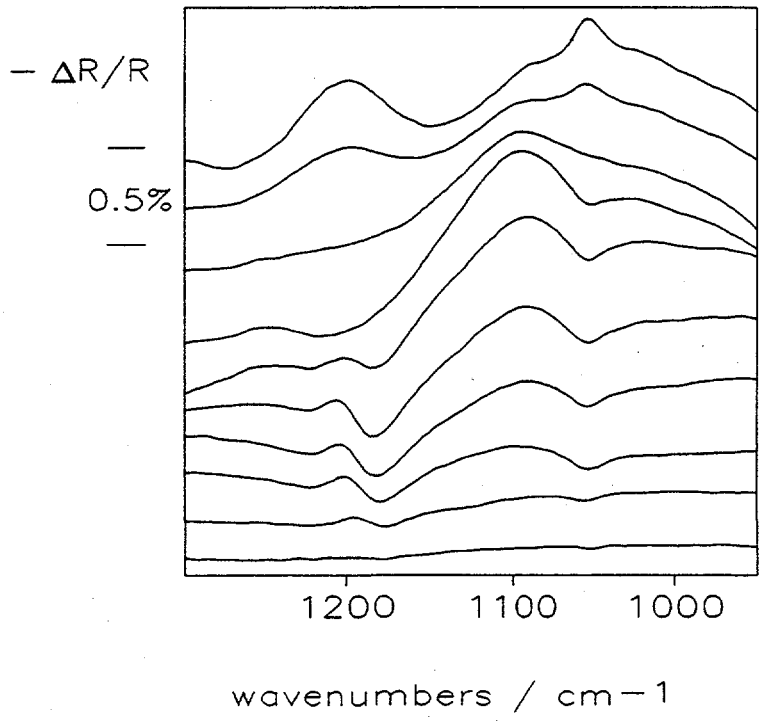

Fig. 6 SNIFTIR spectra from Pt(111) in 0.05M H_2SO_4 with 1mM Ag^+ at sample potentials from 0.7 to 1.15V incremented by 50mV. Reference potential 0.68V; *p*-polarization.

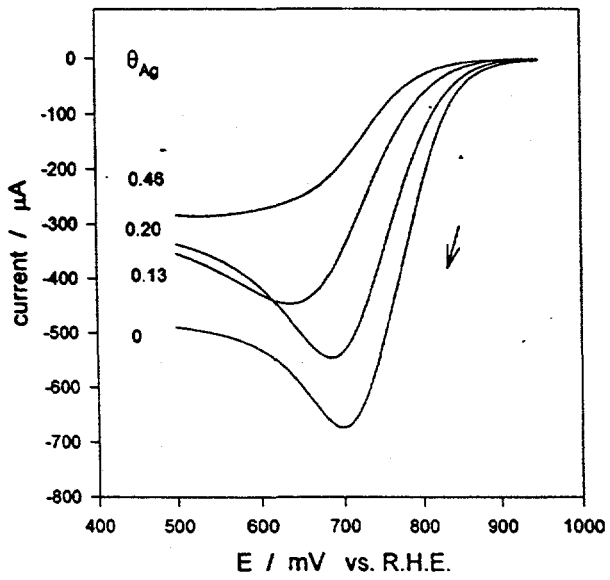

Fig. 7 O_2 reduction on Pt(111) in 0.05M H_2SO_4 as a function of Ag coverage.

O_2 "BRIDGE" O_2 ON-TOP

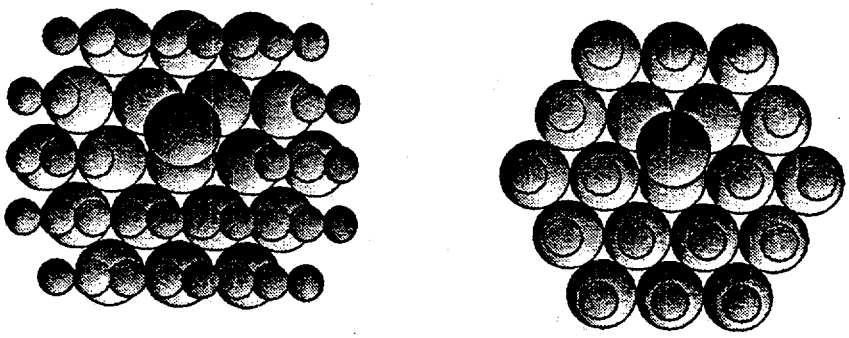

Fig. 8 Models of the site-exclusion by Ag atom for the "bridge' and on-top O_2 adsorption.

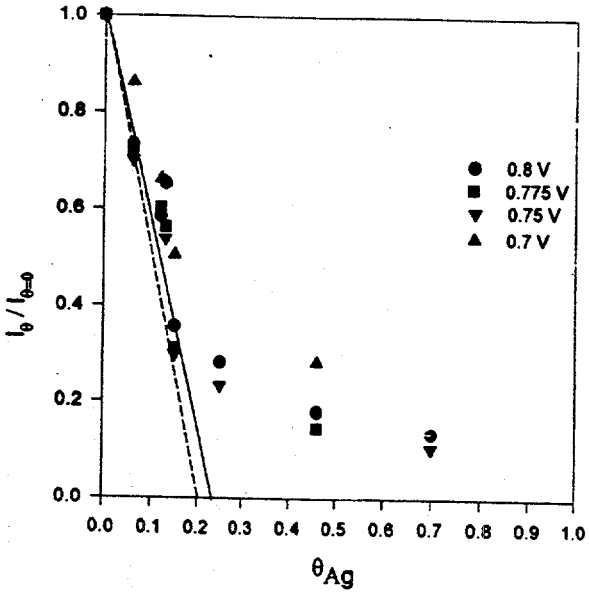

Fig. 9 Normalized O_2 reduction current as a function of Ag coverage at 4 potentials. Solid line: extrapolation at low coverages; dashed line: extrapolation of the calculated curve.